View metadata, citation and similar papers at core.ac.uk
brought to you by CORE
provided by Juelich Shared Electronic Resources

Variation of nonequilibrium processes in p+Ni system with beam energy

A.Budzanowski,[1] M.Fidelus,[2] D.Filges,[3] F.Goldenbaum,[3] H.Hodde,[4] L.Jarczyk,[2] B.Kamys,[2,*] M.Kistryn,[1] St.Kistryn,[2] St.Kliczewski,[1] A.Kowalczyk,[2] E.Kozik,[1] P.Kulessa,[1,3] H.Machner,[3] A.Magiera,[2] B.Piskor-Ignatowicz,[2,3] K.Pysz,[1,3] Z.Rudy,[2] R.Siudak,[1,3] and M.Wojciechowski[2]

(PISA - **P**roton **I**nduced **S**p**A**llation collaboration)

[1] *H. Niewodniczański Institute of Nuclear Physics PAN, Radzikowskiego 152, 31342 Kraków, Poland*
[2] *M. Smoluchowski Institute of Physics, Jagellonian University, Reymonta 4, 30059 Kraków, Poland*
[3] *Institut für Kernphysik, Forschungszentrum Jülich, D-52425 Jülich, Germany*
[4] *Institut für Strahlen- und Kernphysik, Bonn University, D-53121 Bonn, Germany*

(Dated: November 27, 2013)

The energy and angular dependence of double differential cross sections $d^2\sigma/d\Omega dE$ were measured for $p, d, t,$ ^{3,4}He, ^{6,7}Li, ^{7,9}Be, and ^{10,11}B produced in collisions of 0.175 GeV protons with Ni target. The analysis of measured differential cross sections allowed to extract total production cross sections for ejectiles listed above. The shape of the spectra and angular distributions indicate the presence of other nonequilibrium processes besides the emission of nucleons from the intranuclear cascade, and besides the evaporation of various particles from remnants of intranuclear cascade. These nonequilibrium processes consist of coalescence of nucleons into light charged particles during the intranuclear cascade, of the fireball emission which contributes to the cross sections of protons and deuterons, and of the break-up of the target nucleus which leads to the emission of intermediate mass fragments. All such processes were found earlier at beam energies 1.2, 1.9, and 2.5 GeV for Ni as well as for Au targets, however, significant differences in properties of these processes at high and low beam energy are observed in the present study.

PACS numbers: 25.40.-h,25.40.Sc,25.40.Ve
Keywords: Proton induced reactions, production of light charged particles and intermediate mass fragments, spallation, fragmentation, nonequilibrium processes, coalescence, fireball emission

arXiv:0909.1436v1 [nucl-ex] 8 Sep 2009

I. INTRODUCTION

One of the most significant questions to be addressed by studies on proton-nucleus collisions is the predictive power of existing models and computer programs used for their realization. The above question is closely related to two following problems: (i) whether all important physical phenomena are taken into consideration, (ii) whether the parameters of the models are adjusted properly. It is well known that neglecting of an important physical phenomenon may be usually "repaired" in a specific case by appropriate adjusting of free parameters of the model. This procedure cannot be, however, extended to a full set of observables for all targets and energies. Thus, a general model must explicitly contain all important physical phenomena.

The traditionally used description of proton induced reactions at GeV energies assumes that the reactions proceed in two steps. The fast, nonequilibrium step in such two-step model consists in an intranuclear cascade of nucleon-nucleon collisions with a possible coalescence of the nucleons into complex particles as it is realized,e.g., by the INCL4.3 computer program of Boudard *et al.* [1]. This stage of the reaction is assumed to lead to an equilibrated, excited residuum of the target, which in the following evaporates particles or/and emits fission fragments. This picture of reactions turned out to be realistic in many situations. It was, however, observed at proton beam energies above several GeV that copious emission of intermediate mass fragments (IMFs), i.e., ejectiles heavier than ^{4}He and lighter than fission fragments, appears (cf., e.g., [2, 3]) what is interpreted as an analogue of the liquid - gas phase transition (cf., e.g., [4, 5] and references therein). The nucleus, which is treated as a liquid, changes then into a mixture of free nucleons, light charged particles – LCPs (particles with $Z \leq 2$) and IMFs, treated as a fog. In this case, ejectiles are emitted by only one source - the slowly moving target spectator.

It was, however, recently found that at proton beam energies 1.2 - 2.5 GeV the IMFs as well as LCPs originating from p+Ni [6] and p+Au collisions [7, 8] are emitted from three sources. They are interpreted as a fireball - fast and hot source consisted of several nucleons - knocked out by the impinging proton, and two slower and colder sources which are believed to be prefragments of the target nucleus appearing due to its break-up caused by strong deformation induced by the fireball emission. The analysis of the experimental data by a traditional model assuming the presence of intranuclear cascade with the possibility to form complex particles due to coalescence, and evaporation from an equilibrated target remnant could not take account for the presence of these sources and could not reproduce the full set of experimental data. On the contrary, the combination of a traditional model with additional inclusion of the emission from the fireball and two other sources, treated within a

*Electronic address: ufkamys@cyf-kr.edu.pl

phenomenological model, led to a perfect description of energy and angular dependencies of all double differential cross sections $d^2\sigma/d\Omega dE$. It is therefore obvious, that in a proper theoretical analysis such phenomena should be taken into consideration.

The question arises on the energy development of the reaction mechanism. It is not clear, whether the same picture of the reaction may be applied to other energies - below and above the studied proton beam energy range; 1.2 - 2.5 GeV. In the present study the investigation of the reaction mechanism of p+Ni collisions is extended to much lower energy E_p=0.175 GeV, which is on the boarder of applicability of the traditional model of an intranuclear cascade followed by an evaporation [1, 9, 10].

To facilitate the comparison of the results from the present study of the reactions in p+Ni system with results of previous investigations at higher energies in the same nuclear system [6], the present paper is organized in a similar way as Ref. [6]. Experimental data are discussed in the next section, the theoretical analysis is described in the third section starting from IMF data and followed by the analysis of LCPs cross sections, the discussion of results is presented in the fourth and the summary with conclusions in the fifth section.

II. EXPERIMENTAL DATA

The experiment was performed with a selfsupporting Ni target of the thickness of about 150 μg/cm^2, irradiated by an internal proton beam of COSY (COoler SYnchrotron) of the Jülich Research Center. The experimental setup and procedure of data taking were in details described in Refs. [8] and [11].

Double differential cross sections $d^2\sigma/d\Omega dE$ were measured at seven scattering angles; 16^0, 20^0, 35^0, 50^0, 65^0, 80^0, and 100^0 as a function of energy of ejectiles for the following isotopes ^{1,2,3}H, ^{3,4}He, ^{6,7}Li, ^{7,9}Be, and ^{10,11}B.

The absolute normalization of the cross sections was achieved by comparing the proton differential cross sections measured in the present experiment at 20^0, 65^0, and 100^0 with the absolutely normalized proton spectra from the experiment of Förtsch *et al.* [12]. A perfect agreement of the shape of the spectra from both experiments as well as an agreement of their angular dependence can be seen in Fig. 1. It is worthy to point out, that the spectra consist of two parts: a low energy part (energy smaller than $\sim$ 20 MeV) - measured only in the present experiment, where the evaporation of protons from excited target remnants after the intranuclear cascade sets in, and high energy tails, which are due to preequilibrium processes. In the traditional, two-step model this part of the spectra is due to the emission of protons from the intranuclear cascade. As it will be discussed below, the same two components - representing particles emitted from the equilibrated nuclear system as well as those from preequilibrium processes - are visible in the spectra of other LCPs and IMFs.

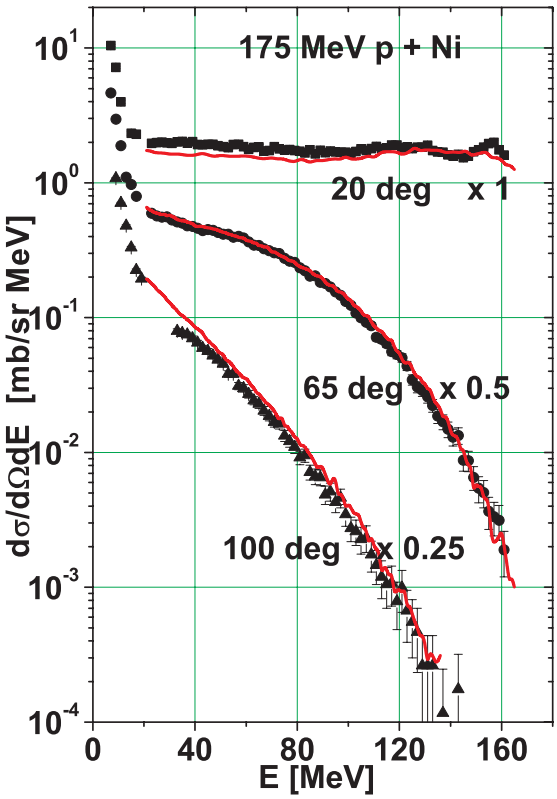

FIG. 1: Proton energy spectra measured at 20^0, 65^0, and 100^0 in the laboratory system. Lines represent the data from Förtsch *et al.* [12], symbols depict the data from the present experiment. The spectra were multiplied by factors written in the figure to avoid overlapping the symbols and lines obtained at different angles.

III. THEORETICAL ANALYSIS

The analysis of present experimental data was performed according to the same procedure as that applied previously to the data from proton induced reactions on Ni target in the work of Budzanowski *et al.* [6] at higher energies.

The experimental data were first compared with calculations performed in the frame of two step model in which the fast stage was calculated as intranuclear cascade with the possibility to coalesce the outgoing nucleons into complex LCPs, and the slow stage was modeled by evaporation of particles (both LCPs and IMFs) from the excited residuum of the intranuclear cascade, which was assumed to be in equilibrium.

The calculations of the first step of the reaction were done using the INCL4.3 computer program of Boudard *et al.* [1], and the calculations of evaporation of particles were realized by means of GEM2 computer program of Furihata [13, 14]. In both types of calculations default values of the parameters, proposed by authors were used,

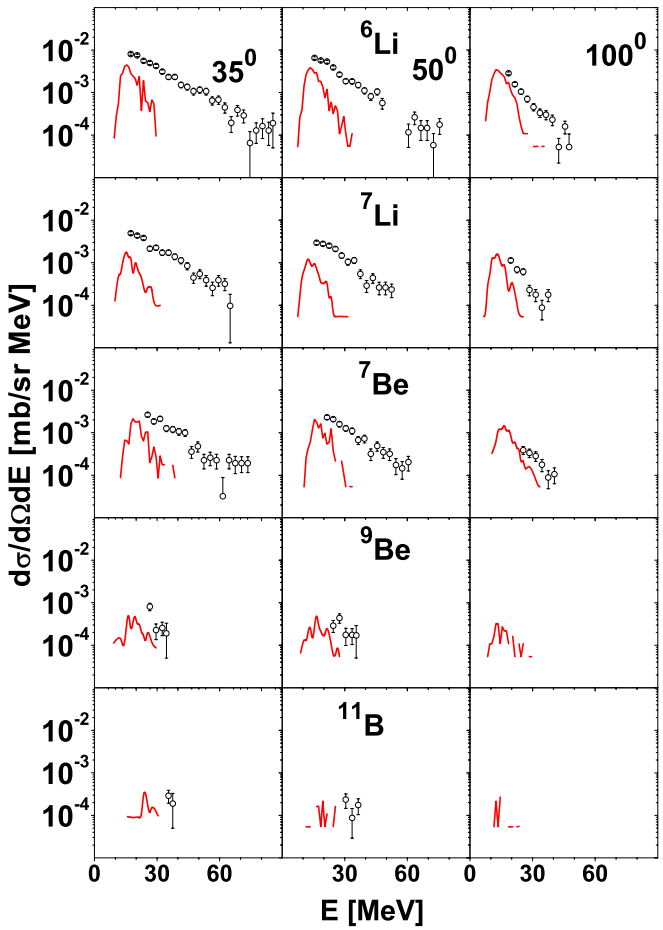

FIG. 2: Typical spectra of selected lithium, beryllium, and boron isotopes from p+Ni collisions measured at 35°, 50°, and 100° (left, middle, and right columns of the figure, respectively) for 0.175 GeV proton beam impinging on to the Ni target. The detected particles are listed in the central panel of each row. Open circles represent the experimental data, and solid lines correspond to intranuclear cascade followed by evaporation of particles, respectively.

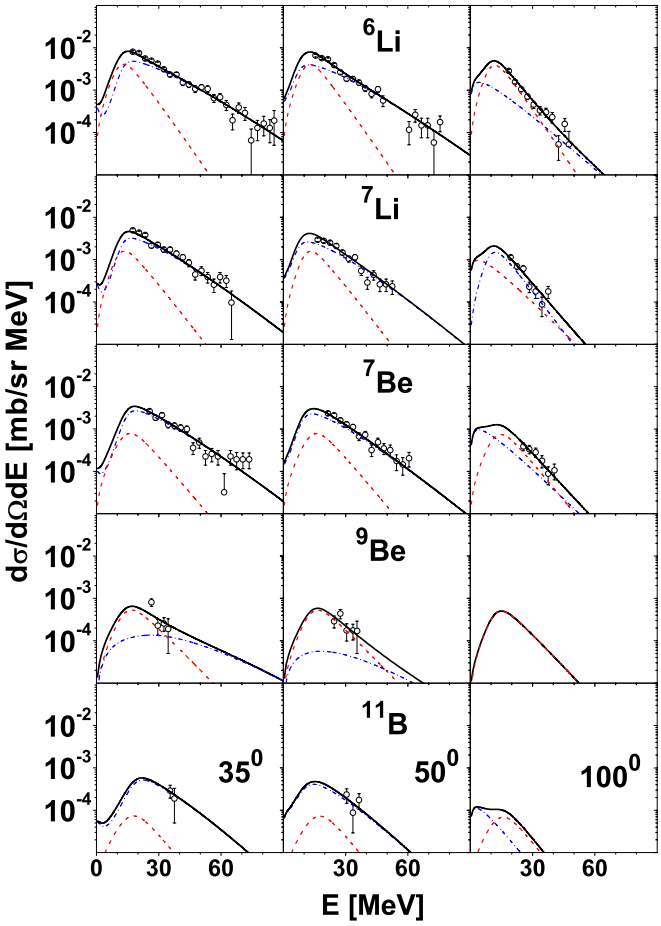

FIG. 3: Same as Fig. 2 but dashed, dot - dashed, and solid lines correspond to slow emitting source, fast emitting source and the sum of both contributions, respectively.

thus no adjusting of the theoretical cross sections to the data was undertaken.

It turned out, that the spectra of both, LCPs and IMFs were not satisfactorily well reproduced. Therefore a phenomenological analysis was performed in which the isotropic emission of particles from sources moving in forward direction (along to the beam) was allowed. Each of the sources had Maxwellian distribution of the energy E available for the two body decay in which the emission of the detected particles occured; $d^2\sigma/dEd\Omega \sim \sqrt{E}\exp(-E/T)$. The velocity of the source - β (in units of speed of light), its temperature - T (in MeV), and the contribution to the total production cross section - σ (in mb) were treated as free parameters.

Two additional parameters, defining the height B of the Coulomb barrier for emitted particles and the diffuseness d of the transmission function through the barrier, were used with fixed values. Further details of the model are described in the Appendix of Ref. [8].

The analysis of IMF data differs from that of LCP cross sections, thus they are described separately below.

A. Intermediate mass fragments

The experimental spectra for ^{6,7}Li, ^{7,9}Be, and ^{11}B measured at 35°, 50°, and 100° scattering angles are shown in Fig. 2 as open dots together with the theoretical calculations performed in the frame of the two-step model (intranuclear cascade followed by evaporation of particles from the excited remnant of the target nucleus), which are depicted by solid lines. The fluctuations of these lines are due to limited statistics of model calculations which were done by the Monte Carlo method and have no physical meaning.

TABLE I: Parameters of two moving sources for isotopically identified IMF's and for ^{4}He: β_i, T_i, and σ_i correspond to source velocity, its apparent temperature, and the total production cross section, respectively. The sum $\sigma \equiv \sigma_1 + \sigma_2$ is also listed. The left part of the Table (parameters with indices "1") corresponds to the slow moving source, and the right part contains values of parameters for the fast moving source.

	Slow source		Fast source					
Ejectile	T_1/MeV	σ_1/mb	β_2	T_2/MeV	σ_2/mb	σ/mb	σ_2/σ	χ^2
^{4}He	7.0(3)	39(3)	0.060(6)	9.7(4)	16.8(2.7)	55.8(4.2)	0.30(6)	32.5
^{6}Li	5.7(4)	0.70(6)	0.045(2)	10.0(2)	0.71(5)	1.41(8)	0.50(5)	1.4
^{7}Li	6.3(8)	0.29(5)	0.041(2)	8.7(4)	0.41(4)	0.70(7)	0.59(8)	1.4
^{7}Be	6.8(1.8)	0.16(7)	0.040(4)	9.0(6)	0.37(6)	0.53(9)	0.70(16)	1.2
^{9}Be	[6.5]	0.12(6)	0.08(2)	[9.0]	0.02(1)	0.14(6)	0.14(7)	1.4
^{10}B	[6.5]	0.10(9)	[0.04]	7.1(3.8)	0.07(4)	0.17(10)	0.42(34)	1.7
^{11}B	[6.5]	0.020(14)	[0.04]	7.0(7.3)	0.06(4)	0.08(5)	0.75(69)	1.3

As can be seen the theoretical spectra are different from the experimental ones in several subjects; (i) the theoretical spectra are almost independent of the scattering angle, whereas the experimental spectra vary with the angle showing increasing of the slope with the scattering angle, (ii) the theoretical spectra are localized at small ejectile energies (smaller than $\sim$ 30 MeV) whereas the experimental spectra cover much larger range of energies, especially for small scattering angles, (iii) the magnitude of the theoretical cross sections is smaller than that of the data.

In the second step of the analysis the emission of IMFs from two moving sources has been calculated adding the cross sections from both sources. The velocity of the fast source β_2, temperature parameters of both sources T_1 and T_2, and total production cross sections σ_1 and σ_2 due to both sources were fitted to obtain the best agreement of the theoretical cross sections with the data for all seven scattering angles simultaneously. The other parameters, i.e., velocity of the slow source β_1 as well as parameters characterizing the Coulomb barrier k_1, k_2 (heights of Coulomb barrier between ejectile and source in units B, i.e. height of Coulomb barrier between ejectile and the target nucleus) and $(B/d)_1$, $(B/d)_2$ were fixed. The velocity of the slow source was assumed to be equal to the average velocity of the residual nuclei after the intranuclear cascade $\beta_1 = 0.0036$ as it was extracted from INCL4.3 calculations, and Coulomb barrier parameters were fixed at arbitrarily chosen values k_1= 0.75, k_2 = 0.3, and $(B/d)_1 = (B/d)_2$=5.5. These parameters almost do not influence the spectra with exception of very low ejectile energies, thus the same values of the parameters were taken as those used at higher beam energies [6]. The experimental spectra measured at 35°, 50°, and 100° (open circles) are shown in Fig. 3 together with results of the calculations (lines). The solid line represents the sum of contributions from both sources, dashed line depicts the cross section originating from the slow source, and dot-dashed line shows cross section corresponding to emission from the fast source.

A very good description of the data has been obtained with the parameters varying smoothly from ejectile to ejectile. The values of the parameters are listed in Table I. The errors of the parameters, estimated by a computer program, which searched for best fit parameters are also given in the Table. Some parameters – closed in square brackets – were fixed during the fit to avoid ambiguities of the parameters, which appear when the data do not put strong enough constraints to the parameters.

As can be seen in Fig. 3, the slow source produces spectra which are almost independent of angle and are similar to those calculated from two-step microscopic model. The fast source contribution to the spectra is angle dependent thus it represents the nonequilibrium process proceeding in the fast stage of the reaction. The spectrum evaluated for this source has a high-energy tail which allows to reproduce the high energy part of the experimental spectra. The relative contribution of this source to the total production cross section is large as can be checked in the Table I (in average it is equal to 53(12)%).

B. Light charged particles

The experimental spectra of LCPs extend to energies higher than 20 - 30 MeV, which is the upper limit of energy for evaporated particles. Thus, it is obvious that the nonequilibrium emission of particles is responsible for the higher energy part of the spectra. In the case of protons, such nonequilibrium emission appears from the intranuclear cascade before achieving an equilibrium in the target residuum. Coalescence of nucleons of the target with the nucleons escaping from the intranuclear cascade, which may proceed if the relative spatial and momentum position of nucleons is small enough, has been considered as the process responsible for emission of complex LCPs. Letourneau *et al.* [15] and Boudard *et al.* [1] proposed to treat the coalescence microscopically during the calculation of an intranuclear cascade. Thus this phenomenon is implemented in the INCL4.3 computer program [1] and therefore this program has been applied in the present work for evaluation of intranuclear cascade and coalescence of nucleons leading to the formation of deuterons,

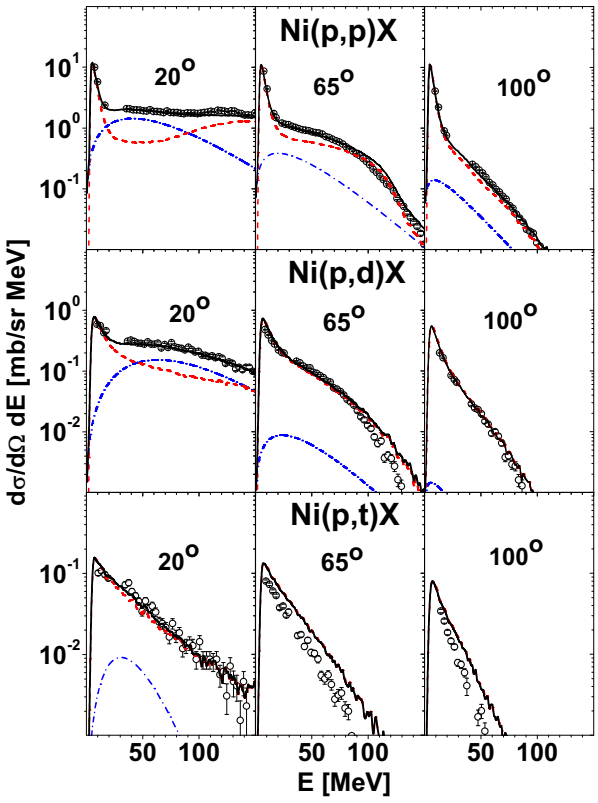

FIG. 4: Typical spectra of protons, deuterons, and tritons (upper, middle, and lower rows of the figure, respectively) measured at 20°, 65°, and 100° (left, middle, and right columns of the figure, respectively) for 0.175 GeV proton beam impinging on to the Ni target. Open circles represent the experimental data, dashed, dot - dashed, and solid lines correspond to two-step model (scaled by factor F - for explanation see text), emission from the fireball and sum of both contributions, respectively. Contribution of the fireball is very small for deuterons emitted at large angles as well as for tritons at all scattering angles.

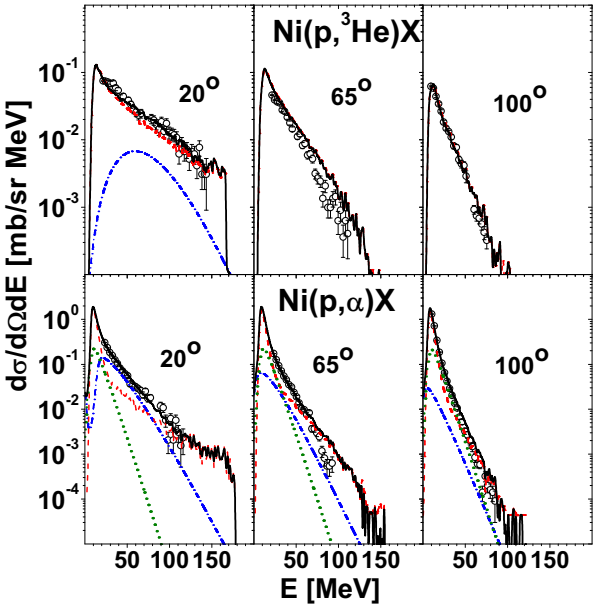

FIG. 5: Typical spectra of ^{3}He and ^{4}He (upper, and lower rows of the figure, respectively) measured at 20°, 65°, and 100° (left, middle, and right columns of the figure, respectively) for 0.175 GeV proton beam impinging on to the Ni target. Open circles represent the experimental data, dashed lines represent results of two-step model (scaled by factor F), and solid line depicts sum of all contributions. Dot-dashed line in the upper panel shows contribution of the fireball whereas the dot-dashed and dotted lines for ^{4}He denote contributions of fast and slow moving sources, respectively.

tritons, ^{3}He and alpha particles. The results of these calculations, coupled with the evaporation of particles evaluated by means of the GEM2 computer program were compared with the experimental spectra. Very good reproduction of triton and ^{3}He spectra was achieved for all scattering angles as well as significant improvement (in comparison to evaporation spectra alone) of deuteron and alpha particle spectra for large scattering angles. However, the small scattering angles of protons, deuterons and alpha particles were still not satisfactorily well reproduced. Moreover, it was found that the improvement of the description of LCPs spectra by inclusion of coalescence deteriorates simultaneously the description of the proton spectra, because increasing of the production of composite particles occurs on the account of decreasing the emission of nucleons.

It was thus assumed that an additional process, namely the emission of a fireball and break-up of the target nucleus, should be taken into consideration as it was found to be necessary for p+Ni and p+Au collisions at higher proton energies (1.2, 1.9, and 2.5 GeV), investigated by present authors (Refs. [6] and [7], respectively). The parameters of the fireball, i.e., its temperature parameter - T_3, velocity of the source - β_3, total production cross section associated with this mechanism - σ_3 were treated as free parameters and modified to obtain the best description of experimental cross sections. Other parameters, i.e., k_3 (the height of the Coulomb barriers in units of B - Coulomb barrier between the ejectile and the target nucleus) and the parameter B/d describing diffuseness of the transmission function through the Coulomb barrier were fixed at arbitrarily assumed values 0.07 and 4.8, respectively. It should be emphasized, that the coalescence and evaporation cross sections were allowed to be scaled down by an adjustable factor F, what physically is understood as making room for new nonequilibrium process, which in original INCL4.3+GEM2 calculations was not considered. Values of the fitted parameters are collected in the Table II.

It turned out that the inclusion of the emission of LCPs from the fireball into the analysis leads to a very good

TABLE II: Parameters β_3, T_3, and σ_3 correspond to the fireball velocity in units of speed of light, its apparent temperature, and the total production cross section, respectively. Parameter F is the scaling factor of coalescence and evaporation contribution extracted from fit to the proton spectra and deuteron spectra. The numbers in parentheses show fixed values of the parameters. The columns described as F$*\sigma_{INCL}$ and F$*\sigma_{GEM}$ contain total production cross sections due to intranuclear cascade with the coalescence and due to evaporation from the target residuum, respectively. The total production cross section obtained by summing of all contributions is depicted in the column denoted by σ. In the case of alpha particles it contains also the contribution of emission from slow and fast sources listed in Table I.

Ejectile	β_3	T_3	σ_3	F	F$*\sigma_{INCL}$	F$*\sigma_{GEM}$	σ	σ_3/σ	χ^2
		MeV	mb		mb	mb	mb		
p	0.232(5)	21.2(1.3)	320(32)	0.83(5)	567	697	1584(32)	0.20(2)	26.8
d	0.240(9)	16.8(2.0)	22.9(3.7)	0.80(3)	104	31	158(5)	0.14(3)	5.3
t	0.142(27)	6.1(4.9)	[0.5]	[0.8]	24.1	2.8	27.4	0.02	14.3
^{3}He	0.205(20)	7.3(3.0)	[0.5]	[0.8]	16.0	4.8	21.3	0.02	18.8
^{4}He				[0.8]	11.5	129	196.3(4.2)		32.5

description of proton and deuteron spectra but it gives only negligible modification of triton and ^{3}He theoretical spectra as it is visible in Figs. 4 and 5. The importance of the fireball contribution to proton and deuteron data may be also judged from ratio of total production cross section of these particles via fireball emission to cross section representing sum of all processes. As can be seen in Table II the relative fireball contribution to proton and to deuteron cross sections is equal to 20(2)% and 14(3)% , respectively. This is a rather small value in spite of the fact that it is crucial for a proper description of the spectra, especially at forward angles. On the contrary, the fireball is practically negligible as concerns the total production cross section of tritons and ^{3}He particles. Its contribution is of order of 2% only. It should be pointed out that the scaling factor F of INCL4.3 and GEM2 cross section was fixed for tritons, ^{3}He, and 4He at the same value as for deuterons, i.e., F=0.8. Some smaller value will perhaps improve the description of the cross sections, since theoretical cross sections of INCL4.3 and GEM2 slightly overestimate the data, however the contribution of the fireball to triton and ^{3}He spectra is very small and thus searching F and fireball cross section σ_3 independently led to ambiguities of parameters.

The alpha particle cross sections need an additional contribution from two moving sources besides the coalescence and evaporation cross sections. The parameters of these sources are different from fireball parameters but are quite similar to those found earlier for IMFs. It can be thus stated, that the alpha particles behave more as IMFs than as LCPs. The same effect has been observed at beam energies over 1 GeV for p+Ni system [6].

IV. DISCUSSION

The velocity and temperature parameters of moving sources for all ejectiles are presented on Fig. 6 in function of the mass of ejectiles. Their values behave in very similar manner as it was observed at higher beam energies in p+Ni [6] and p+Au [7] systems, i.e., they belong to three well separated sets, representing the slow source (β_1 and T_1), the fast source (β_2 and T_2), and the fireball (β_3 and T_3). The ejectile mass dependence may be approximated by straight line for each source with a slope which is larger for the fireball than for the fast source. A velocity of the source can be also dependent on the mass of the ejectile because mass of the source may vary for different ejectiles.

As it was discussed in the previous paper dealing with reactions in p+Ni system at higher energies [6], the linear dependence of the temperature parameter on the mass of ejectiles can be used for an estimation of mass of the source. The parameters of linear functions describing dependence of the temperature parameter T and velocity β of three sources on the ejectile mass A are collected in Table III. The velocity of the slow source has been fixed at 0.0036 c, i.e., at an average velocity of residua of intranuclear cascade extracted from INCL4.3 calculations. The temperature of this source was also found to be independent of the mass of ejectile and may be represented by its average value $\sim$ 6.5 MeV.

The small and not well defined slope of the mass dependence of the temperature for the fast source and the fireball give very crude estimation of their masses, i.e., 45(33) and 4.2(1.0) mass units, respectively. The former mass value has too large error to be used for any further reasoning. The latter value, apart from being not well determined, is smaller than the mass of the fireball extracted from high energy data, i.e., 5.5(3) mass units [6]. Such decreasing of the mass of the fireball seems to be in accord with the fact that only proton and deuteron spectra have significant contribution of emission from the fireball at 0.175 GeV beam energy, whereas at higher energies such a contribution was quite large also for tritons and ^{3}He particles.

The next important difference concerns the values of temperature parameters. The temperature parameters at low beam energy are approximately two times smaller than appropriate parameters determined at high energies. This seems to be a natural consequence of the fact that the excitation energy of the target increases with

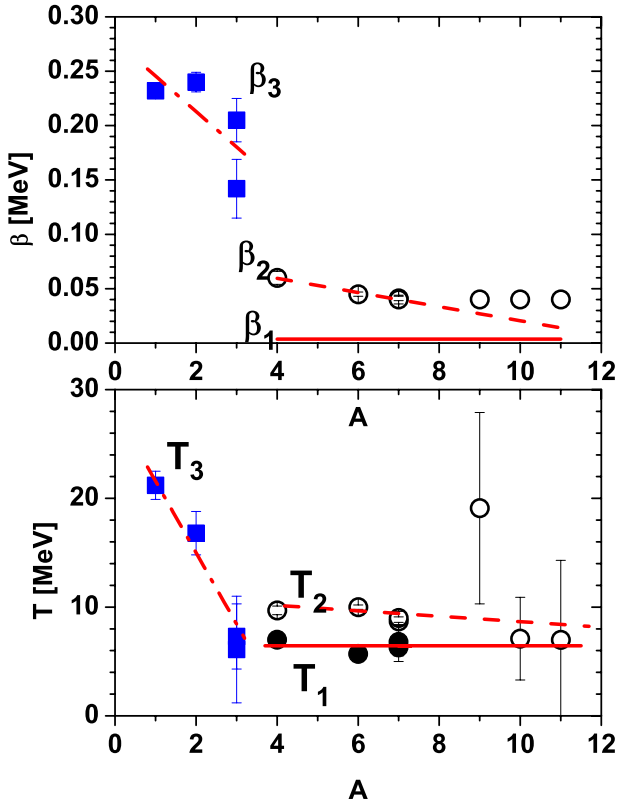

FIG. 6: In the lower panel of the figure the apparent temperature of the moving sources is drawn as a function of the ejectile mass A. Open circles and full dots represent values of temperature parameters T_2 and T_1 for fast and slow source, respectively. Full squares indicate temperature T_3 of the fireball. The solid and dashed lines were fitted to the points representing the lightest IMF's: ^{6}Li, ^{7}Li, ^{7}Be, and ^{4}He. Dash dotted line was fitted to points representing the LCP's. In the upper panel of the figure the dependence of the velocity of the sources is drawn versus the mass of ejectiles. The symbols and lines have the same meaning as for the lower part of the figure with one exception: The full dots are not shown because the velocity of the slow source was fixed during the analysis (at velocity β_1=0.0036) and it is represented by the solid line in the figure.

the beam energy since, at approximately the same rate of the energy transfer, the total transferred energy must be larger at higher beam energy. The same reasoning can be applied to the increase of the momentum transfer from projectile to the target, which mainly determines the velocity of the target residuum after the intranuclear cascade. According to intranuclear cascade calculations the velocity of target residuum at low beam energy, i.e. 0.175 GeV is equal to 0.0036 c, whereas at high energies it is larger, i.e., equal to 0.0050 c, and is almost independent of energy in the range 1.2 - 2.5 GeV.

The interesting observation, contradicting to the above reasoning is, that *the velocities of the fast source as well as of the fireball found from the fit are significantly larger*

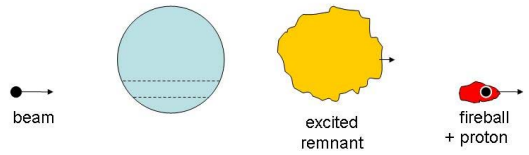

FIG. 7: Fireball emission from Ni target at 0.175 GeV beam energy.

at 0.175 GeV beam energy than at higher beam energies. This may indicate, that properties of the reaction mechanism at low energy are different than those at 1.2 - 2.5 GeV.

According to the present phenomenological model the sources of ejectiles move along the beam, thus the momentum conservation requires that the *algebraic* sum of momenta of all sources should be equal to projectile momentum (p_b=0.60 GeV/c). Assuming that the fitted values of the fireball velocity β_3 for p, d, t, and ^{3}He are not biased by errors it is possible to estimate the maximal mass of the fireball – 2.7 mass units – which assures that the momentum of the fireball emitting all these particles is not larger than the beam momentum. Assuming the mass of the fireball not larger than 3 mass units excludes the possibility of emission of tritons and ^{3}He, what is compatible with the fact that contribution of the fireball found from the fit to spectra of these particles is negligibly small. Furthermore, the emission of protons and deuterons is possible from such a three-nucleon fireball but then their momenta evaluated with velocities β_3 of Table II exhaust full available momentum: $p(fireball_p)$=0.65 GeV/c, $p(fireball_d)$=0.68 GeV/c. The quoted above momenta are even slightly larger than the beam momentum p_b, but the fact that the fireball velocity was found from unconstraint fit and is biased by errors, the agreement of momenta of the fireballs emitting protons and deuterons with the beam momentum is quite good. Thus, presence of 3-nucleon fireball emitting protons and/or deuterons is in agreement with momentum conservations and shows that *full beam momentum is transferred to the fireball.* This specifically means that: (i) *The proton from the beam cannot fly away separately from the fireball*, (ii) *the creation of a fireball cannot simultaneously lead to break-up of the rest of the target.*

The fact, that two sources, heavier than the fireball are observed in the analysis of IMFs means that a break-up of the target occurs. Since the fireball emission cannot be accompanied by the break-up, *the break-up must proceed without fireball emission.* It is worthy to mention, that such a capture of the projectile leading to excitation of the nucleus without emission of the fireball, has been discussed by Aichelin et al. [16]. They estimated that protons of energies smaller than 0.2 - 0.25 GeV should be captured without sending the fireball. The

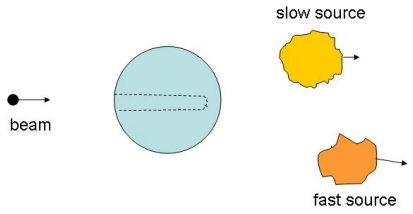

FIG. 8: Break-up of Ni target at 0.175 GeV beam energy.

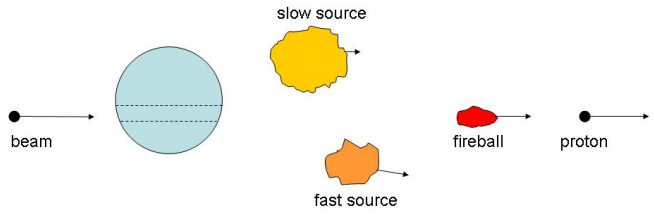

FIG. 9: Fireball emission from Ni target at high beam energy (over 1 GeV).

excited nucleus, created during such a process may deexcite by emission of particles, in similar way as the heavy residuum of the intranuclear cascade, but may also break up, what leads to the emission of two excited sources of particles as it is in our picture of the reaction mechanism.

The fireball emission and the break-up of the target, illustrated by Figs. 7 and 8, may appear at low energy, e.g. 0.175 GeV, only exclusively. It is important to emphasize that, nevertheless, both are observed in the analyzed data. This may be connected with the fact that at different impact parameters the straight way of the proton through the target has different length. The peripheral collisions correspond to shorter way through the nucleus, i.e., to the smaller stopping power, whereas the central collisions, on the contrary, to the longest way and the strongest stopping power. The estimation of Aichelin et al. [16] should be, thus, treated as done for a specific case - for central collisions.

The proton impinging with high kinetic energy, e.g., 1.2 GeV or higher, can move through the nucleus knocking-out a fireball, but relative momentum of the proton and the fireball may be so large, that the proton flies independently of the fireball. Then the momentum of the fireball is smaller than the momentum of the beam, and it is not related to the beam momentum in an unambiguous manner. This may be a reason why the velocity of the fireball, observed in p+Ni collisions in the proton energy range from 1.2 to 2.5 GeV [6], is smaller than that observed at 0.175 GeV. Moreover, it does not change significantly, in contrast to strong variation of the beam energy.

A schematic presentation of this reaction mechanism is shown in Fig. 9 for p+Ni collisions at energies above $\sim$ 1 GeV.

TABLE III: Temperature and velocity parameters of three sources of ejectiles for Ni target. In the second column the parameters obtained in the present study at a beam energy of 0.175 GeV are shown, whereas the third column presents parameters averaged over beam energies 1.2, 1.9, and 2.5 GeV from [6]. T denotes apparent source temperature (in MeV), τ - the temperature parameter corrected for the recoil, A_S represents mass number of the source, and β its velocity in units of speed of light. The symbol A indicates the mass number of the ejectile. Parameters with index 1 correspond to slow source, with index 2 to fast source, and with index 3 to the fireball.

Parameter	Ni(0.175 GeV)	Ni(1.2 - 2.5 GeV)
T_1	6.5(3)	11.2(7) - 0.4(2) $*$ A
τ_1	6.5(3)	11.2(7)
A_{S_1}	?	28(15)
β_1	[0.0036]	[0.005]
T_2	11.2(1.0) - 0.25(17) $*$ A	22.5(6) - 0.8(1) $*$ A
τ_2	11.2(1.0)	22.5(6)
A_{S_2}	45(33)	28(4)
β_2	0.059(5) - 0.0034(6) $*$ A	0.044(6) - 0.0021(7) $*$ A
T_3	28.1(2.3) - 6.6(1.4) $*$ A	52.7(1.1) - 9.6(4) $*$ A
τ_3	28.1(2.3)	52.7(1.1)
A_{S_3}	4.2(1.0)	5.5(3)
β_3	0.278(56) - 0.033(23) $*$ A	0.209(11) - 0.053(5) $*$ A

V. SUMMARY AND CONCLUSIONS

The double differential cross sections $d^2\sigma/d\Omega dE$ for the production of ^{1,2,3}H, ^{3,4}He and light IMFs (^{6,7}Li, ^{7,9}Be, ^{10,11}B) in collisions of proton with a Ni target hasve been measured at 0.175 GeV beam energy. The aim of the study was to investigate whether the nonequilibrium processes, which were found to play an important role at higher energies (1.2, 1.9, and 2.5 GeV) [6] are also present at such low energy as 0.175 GeV.

The data were analyzed using a two-step microscopic model. The first step of the reaction was described as the intranuclear cascade of nucleon-nucleon collisions initiated by the proton from the beam. It was allowed that during the intranuclear cascade the coalescence of nucleons into complex LCPs may proceed. An emission of nucleons from the cascade as well as an emission of LCPs created due to the coalescence was the only nonequilibrium process taken explicitely into consideration by this model. The second step of the reaction was assumed to be described as an evaporation of particles (nucleons, LCPs and IMFs) from the equilibrated target residuum after the intranuclear cascade. It was found that main properties of the spectra of LCPs are well reproduced by the model with the exception of forward scattering angles in proton and deuteron channels as well as all angles in the alpha particle channel. The IMF spectra were also not satisfactorily reproduced, especially for high energy IMFs.

It is worthy to point out that a good quality of descrip-

tion of triton and ^{3}He spectra by coalescence of nucleons and evaporation was achieved with INCL4.3 and GEM2 computer programs, which used default values of the parameters. Such a good agreement of theoretical cross sections with the data measured at 0.175 GeV beam energy is astonishing, because – according to authors of the program [1, 10] – the present beam energy is on the boarder of energy range where the concept of intranuclear cascade is applicable.

A phenomenological analysis was performed assuming that additional processes appear, which may be simulated by the emission from three moving sources as it was successfully done at higher energies. It was found that the cross sections of proton and deuteron emission can be very well described when the emission from fireball, i.e., fast and hot source moving in the forward direction, was taken into account. The contribution of this process to the total production cross sections is rather small - 20% for protons and 14% for deuterons, however, it significantly improves description of the spectra at forward angles. Good reproduction of triton and ^{3}He spectra by two-step process, where the coalescence of nucleons was very important, did not need any significant contribution of other nonequilibrium processes. The description of alpha particle spectra as well as IMF spectra was very improved by inclusion of emission from two moving sources, which were interpreted as prefragments of the target nucleus created due to break-up of this nucleus caused by an impinging proton.

Due to a very good description of energy and angular dependencies of differential cross sections $d^2\sigma/d\Omega dE$ it was possible to extract total production cross sections for all investigated ejectiles. These cross sections are listed in Tables I and II for IMFs and LCPs, respectively.

The discussed above picture of the reaction mechanism agrees generally with the picture of the nonequilibrium reactions investigated at higher beam energies. There were, however, found specific properties of the nonequilibrium reactions appearing at 0.175 GeV but not observed at high energies: (i) The fireball exhausts the total available momentum, thus it cannot be accompanied by break-up of the target remnant, (ii) The break-up of the target appears due to capture of the proton without emission of the fireball.

Acknowledgments

The technical support of A.Heczko, W. Migdał, and N. Paul in preparation of experimental apparatus is greatly appreciated. This work was supported by the European Commission through European Community-Research Infrastructure Activity under FP6 "Structuring the European Research Area" programme (Hadron Physics, contract number RII3-CT-2004-506078 as well as the FP6 IP-EUROTRANS FI6W-CT-2004-516520). One of us (MF) appreciates financial support of Polish Ministry of Science and Higher Education (Grant No N N202 174735, contract number 1747/B/H03/2008/35). This work was also partially supported by the Helmholtz Association through funds provided to the virtual institute "Spin and strong QCD" (VH-VI-231).

[1] A. Boudard, J. Cugnon, S. Leray, and C. Volant, Nucl. Phys. A **740**, 195 (2004)
[2] J. Richert, P. Wagner, Physics Reports 350, 1 (2001)
[3] V.E. Viola, K. Kwiatkowski, L. Beaulieu, D.S. Bracken, H. Breuer, J. Brzychczyk, R.T. de Souza, D.S. Ginger, W-C. Hsi, R.G. Korteling, T. Lefort, W.G. Lynch, K.B. Morley, R. Legrain, L. Pieńkowski, E.C. Pollacco, E. Renshaw, A. Ruangma, M.B. Tsang , C. Volant, G.Wang, S.J.Yennello, N.R.Yoder, Physics Reports 434, 1 (2006)
[4] V. A. Karnaukhov, H. Oeschler, S. P. Avdeyev, E. V. Duginova, V. K. Rodionov, A. Budzanowski, W. Karcz, O. V. Bochkarev, E. A. Kuzmin, L. V. Chulkov, E. Norbeck, and A. S. Botvina, Phys. Rev. C **67**, 011601(R)(2003)
[5] V. A. Karnaukhov, H. Oeschler, S. P. Avdeyev, V. K. Rodionov, V. V. Kirakosyan, A. V. Simonenko, P. A. Rukoyatkin, A. Budzanowski, W. Karcz, I. Skwirczyńska, E. A. Kuzmin, L. V. Chulkov, E. Norbeck, and A. S. Botvina Phys. Rev. **C** 70, 041601(R)(2004)
[6] A. Budzanowski et al., arXiv:0908.4487 [nucl-ex] 31 Aug 2009 and to be published
[7] A. Budzanowski, M. Fidelus, D. Filges, F. Goldenbaum, H. Hodde, L. Jarczyk, B. Kamys, M. Kistryn, St. Kistryn, St. Kliczewski, A. Kowalczyk, E. Kozik, P. Kulessa, H. Machner, A. Magiera, B. Piskor-Ignatowicz, K. Pysz, Z. Rudy, R. Siudak, and M. Wojciechowski, Phys. Rev. C **78**, 024603 (2008)
[8] A. Bubak, A. Budzanowski, D. Filges, F. Goldenbaum, A. Heczko, H. Hodde, L. Jarczyk, B. Kamys, M. Kistryn, St. Kistryn, St. Kliczewski, A. Kowalczyk, E. Kozik, P. Kulessa, H. Machner, A. Magiera, W. Migdał, N. Paul, B. Piskor-Ignatowicz, M. Puchała, K. Pysz, Z. Rudy, R. Siudak, M. Wojciechowski, and P. Wüstner, Phys. Rev. C **76**,014618 (2007)
[9] J. Cugnon, Nucl. Phys. **A**, 751 (1987)
[10] J. Cugnon, C. Volant, S. Vuillier, Nucl. Phys. **A**, 475 (1997)
[11] R. Barna, V. Bollini, A. Bubak, A. Budzanowski, D. D.Pasquale, D. Filges, S. V. Förtsch, F. Goldenbaum, A. Heczko, H. Hodde, A. Italiano, L. Jarczyk, B. Kamys, J. Kisiel, M.Kistryn, St. Kistryn, St. Kliczewski, A. Kowalczyk, P. Kulessa, H.Machner, A. Magiera, J.Majewski, W.Migdał, H.Ohm, N.Paul, B. Piskor-Ignatowicz, K. Pysz, Z. Rudy, H. Schaal, R. Siudak, E. Stephan, G.F.Steyn, R.Sworst, T.Thovhogi, M.Wojciechowski, W.Zipper, Nucl. Instr. Meth. in Phys. Research A **519**, 610 (2004)
[12] S.V. Förtsch, A.A. Cowley, J.J. Lawrie, D.M. Whittal, J.V. Pilcher, and F.D. Smit, Phys. Rev. **C** 43, 691 (1991)
[13] S. Furihata, Nucl. Instr. and Meth. in Phys. Research B

71, 251 (2000)
[14] S. Furihata and T. Nakamura, Journal of Nuclear Science and Technology Supplement **2**, 758 (2002)
[15] A. Letourneau, A. Böhm, J. Galin, B. Lott, A. Péghaire, M. Enke, C. M. Herbach, D. Hilscher, U. Jahnke, V. Tishchenko, *et al.*, Nucl. Phys. A **712**, 133 (2002)
[16] J. Aichelin, J. Hüfner, and R. Ibarra, Phys. Rev. C **30**, 107 (1984)